Desalination and Water Treatment
www.deswater.com
doi: 10.5004/dwt.2023.29894

309 (2023) 93–104
October

Implementation and design of an electrical characterization system for membrane capacitive deionization units in water treatment, with teaching purpose

F.A. Leon-Zerpa*, J.J. Santana-Rodriguez, A. Ramos-Martin, C.A. Mendieta-Pino, V. Henriquez-Concepcion

Process Engineering Department, University of Las Palmas de Gran Canaria, Tel.: 0034686169516; emails: federico.leon@ulpgc.es (F.A. Leon-Zerpa), david.santana122@alu.ulpgc.es (J.J. Santana-Rodriguez), alejandro.ramos@ulpgc.es (A. Ramos-Martin)

Received 28 June 2023; Accepted 23 August 2023

ABSTRACT

The desalination of seawater is one of the most established techniques in the world. In the middle of the 20th century using water evaporation systems, later with reverse osmosis membranes and nowadays the possibility of capacitive deionization membranes. Capacitive deionization is an emerging technology that makes it possible to obtain drinking water with an efficiency of 95%. This technology is in the development stage and consists of porous activated carbon electrodes, which have great potential for saving energy in the water desalination process, and which can be used for desalination process, using an innovative technology called capacitive deionization. A prototype has been designed and can operate with constant current charging and discharging. Adequate precision has been achieved, as can be seen in the results obtained. A philosophy of using free software with open-source code has been followed, such as: the Arduino and Processing Programming Editors; as well as the Arduino Nano Board, the analog-to-digital converter and the Adafruit digital-to-analog converter. Moreover, a low-cost system has been developed. A robust and versatile system has been designed for water treatment, and a flexible system has been obtained for the specifications established as it is shown in the results section.

Keywords: Membranes; Capacitive deionization; reverse osmosis; desalination

1. Introduction

The desalination of seawater is one of the most established techniques in the world. In the middle of the 20th century using water evaporation systems and later with reverse osmosis membranes, however the high energy consumption, generally through fossil fuels, has been an important issue to solve [1–3].

Nowadays, it is introduced the possibility to pass from the reverse osmosis to the capacitive deionization, which is a novel system still under development that, in addition to remove salt from the water, allows to store energy.

Currently, some media outlets are claiming that the current hydrological year is the driest hydrological year of the decade. In the last 12 months, the Spanish water reserve has decreased by a volume of water equivalent to that of the Ebro basin (7,511 hm^3 of capacity).

These phenomena are aggravated by the evident signs of climate change and, in countries such as Spain, by the advance of desertification processes in large areas, causing water to become an essential resource that water has become as precious a commodity as oil [4].

Knowing that 97% of the planet's water is salty, the desalination of brackish or marine water is one of the possible or seawater desalination is one of the possible alternatives to mitigate the problem. However, current desalination technologies such as: reverse osmosis and distillation,

* Corresponding author.

Presented at the European Desalination Society Conference on Desalination for the Environment: Clean Water and Energy, Limassol, Cyprus, 22–26 May 2023

1944–3994/1944–3986

present a serious problem, which is high energy consumption to produce water drinkable, as well as the problem of boron removal.

Capacitive deionization is an emerging technology that makes it possible to obtain drinking water with an efficiency of 95%. This technology is in the development stage and consists of porous activated carbon electrodes, which have great potential for saving energy in the water desalination process, and which can be used for desalination process, using an innovative technology called capacitive deionization (CCD). In CCD, salt ions are removed from brackish water by applying a voltage difference between two porous electrodes in which the ions are temporarily immobilized, and dissolved salts are removed from different types of water.

Design and implementation of a characterization system for capacitive deionization units for water treatment, types of water, ranging from supply water to water from industrial processes. Capacitive deionization has emerged over the years as a robust, energy-efficient solution for water treatment. An effective technology for desalination of water with low to moderate salt content [5].

Finally, the optimal operating regime is obtained for water with a salt concentration of slightly less than 10 g/L. This is since salt ions are minority compounds in the water, so that they are in the water, so they can be removed from the mixture with this technology. In contrast, other methods mostly extract the water phase from the salt solution. This technology also allows for the possibility of integrating renewable energy sources and energy storage [6–10].

The main objective of this study is the design and implementation of a characterization system for capacitive deionization units in water treatment. It is also intended to make use of this system to obtain results that will make it possible to analyse the impact of this technique on different CCD elements. The electrical characterization of the CCD system has been implemented [11–13]. Although in more detail the objectives to be achieved are the following:

(a) To study a control system with a microcontroller that will allow interaction, control, conditioning of different tests and data collection with the medium.
(b) To study the variation of the concentration due to the influence of injecting energy into the system, being influenced by the pH of the solution, temperature, conductivity, etc.
(c) Analyse by numerical methods the variables involved in the system.
(d) Develop a system capable of testing different situations that verify the tests described in the articles consulted.
(e) Establish a laboratory-scale electrochemical evaluation methodology for the ILC. In addition to the tests, the results obtained will be used to determine improvements in active materials (activated carbon, carbon fibers, carbon aerogels, etc.) will be determined from the results obtained and current collectors that make up the electrodes.
(f) The battery of results generated will serve as didactic material to illustrate the influence of the effects studied. This material will be useful for future students and teachers of the School of Industrial and Civil Engineering of the University of Las Palmas de Gran Canaria with the research and improvements of the CCD.

2. Materials and methods

Compared to the classical working modes of the 20th century there have been several innovations and new technologies such as: ion-exchange in the membrane (Fig. 1) [14–18]; and operational optimization in modes such as: "stop-flow" during ion exchange [19], salt ratio upon voltage reversal [16], current constant during operation [19], energy recovered for desalination in relation to cycling [20,21], flow through electrostatic where water is directly faced through the electrostatic [22,23] and flow electrodes based on suspended carbon [24].

Regarding the historical evolution of CCD, a stage is defined before 1995, when aerogel carbon was developed for CCD. The peons who worked with the desalination concept called it "electrochemical water demineralization" and its originator was Blair and Murphy [25], Arnold and Murphy [26], Murphy et al. [27] and Murphy and Caudle [28–31]. The basic standardized methods for supercapacitors have been used to study the behavior of the CDI (Capacity De-Ionization) [32,33]. These methods are constant current charging and discharging, constant power cycling, cyclic voltammetry, and electrochemical impedance spectrometry. These procedures and the self-charging and self-discharging phenomena will be classified into three typologies: frequency, dynamic and energy characterization.

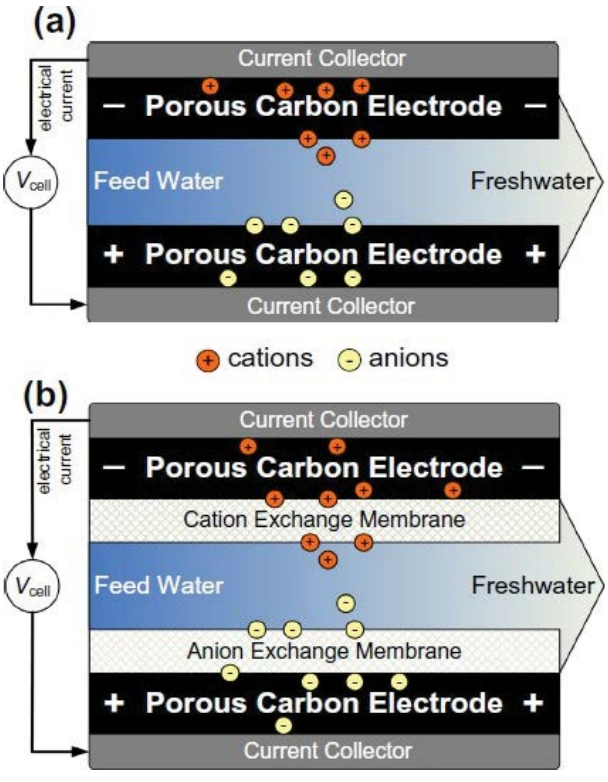

Fig. 1. Membrane cell model circuit (capacitive deionization) [10].

2.1. Frequency characterization

The electrochemical impedance spectroscopy (EIS) method is used to characterize the electrochemical behavior of energy storage devices.

This method has gained popularity in the last decade, especially in the determination of the capacity in fuel cells and batteries due to the development of the electric car [34,35].

The purpose of the EIS is to study the system response to the application of a small amplitude periodic alternating current (AC) signal, these measurements are carried out at different frequencies, which is why it is in the group of frequency characterization; however, this technique is very sensitive, and it is essential to do it as accurately as possible. Therefore, it is necessary to use several characterization techniques because there is no single technique that gives all the expected results. Complementary techniques are therefore used.

On the other hand, there are limitations at high frequencies with the CCD due to the low impedance that the CCD cell can present. One of the factors conditioning the impedance of the CCD is dissolution, others are caused by coupling effects between the power supply and the media system cables [36]. These adversities are limited to low frequencies. In practice, twisted cables are used for the measurement cells to reduce these types of errors.

2.2. Dynamic characterization

The constant current charge/discharge method is the simplest method to apply with direct current (DC), it analyses the response of the CDI when a constant charge/discharge current is applied to it. Despite being a basic method, it is widely used in the characterization of capacitors. Its application is documented with standardizations and will be the main object of the characterization of the CDI in this work, being the main endorsement of the designed device [37–40].

The self-charging or self-discharging of the CDI has its origin in two main causes. First, when the CDI is charged or discharged, there is a diffusion of ions from the solution to the activated carbon electrode, or vice versa. The diffusion immediately after charging or discharging causes a self-discharge or self-charge, respectively. Secondly, these phenomena exist due to leakage current. Self-discharge by diffusion occurs predominantly in the initial stage, however, self-discharge by leakage is significant after self-discharge begins [41]. Self-discharge originates during dynamic operation, for example, the dynamic operating cycle of electric vehicles [42], whose genome is through the equivalent impedance method whose phase element is constant.

On the other hand, we highlight cyclic voltammetry (CV), which has achieved the distinction of a procedure to evaluate the performance of energy storage systems, as well as to determine the life cycle, the effects of internal resistance and dissipation losses [43]. The method consists of applying a linear voltage ramp, storing the current response in the capacitors, this current is directly associated with the capacity of the component achieving a versatile procedure [44–49].

Constant power cycling is known as "cycle life testing" (CLT); it is a methodology for calculating the electrochemical device parameter based on periodic charging and discharging, separated by rest time intervals [50–53].

The procedure consists of charging the device at a given power until a voltage is achieved [54–57]. Once this point is reached, the polarity of the current is reversed by applying a given value, and the current is resumed by reversing the current, so that the charging cycle is continued up to a higher voltage [45,46].

This is a research study in the industrial field and several milestones have been previously established, which are as follows:

(1) A device capable of characterizing capacitive deionization for different tests, shown in Fig. 2, in such a way that the main characteristics of capacitive deionization can be obtained, such as equivalent series resistance, capacitance, etc.
(2) A system capable of collecting the test parameters and configuring it through a graphical user interface (GUI).
(3) A procedure capable of characterizing the CCD for stationary flows.
(4) The results obtained will be studied in future research lines for CCD technology.

2.3. General description of the system

Fig. 3 shows the basic block diagram of the CCD characterization system and Fig. 4 the interrelation of blocks. These blocks that make up this diagram define the genome of the system. It is briefly explained below:

(1) ***Control and data acquisition system***: this part of the system can store data and control the different parameters of the CDI. This part of the system can analyse the data in real time to actuate the power system, attack cell control; the system offers a flexible and versatile solution, with respect to traditional systems.
(2) ***Power system***: it is responsible for feeding the attack cell to the CDI so that it can operate correctly.
(3) ***Transducers***: their task in the system is to transform or adapt a signal of any kind to the inputs and outputs. The device has been differentiated into two parts: actuators and sensors, both of which communicate with the control and data acquisition system. The actuators generate changes in the power system. The sensors, on the other hand, continuously evaluate the status of the parameters of the CDI to be characterized, so that there is feedback that closes the circuit and allows the correct operation of the device.
(4) ***CDI***: this is the object of study of this TFM. Its correct operation is essential to characterize it. Its operating range has been designed to satisfy the needs required in the programmed tests.

3. Results

The target prototype developed for characterization testing shall be capable of charging and discharging at constant voltage and current. In addition, the power supply

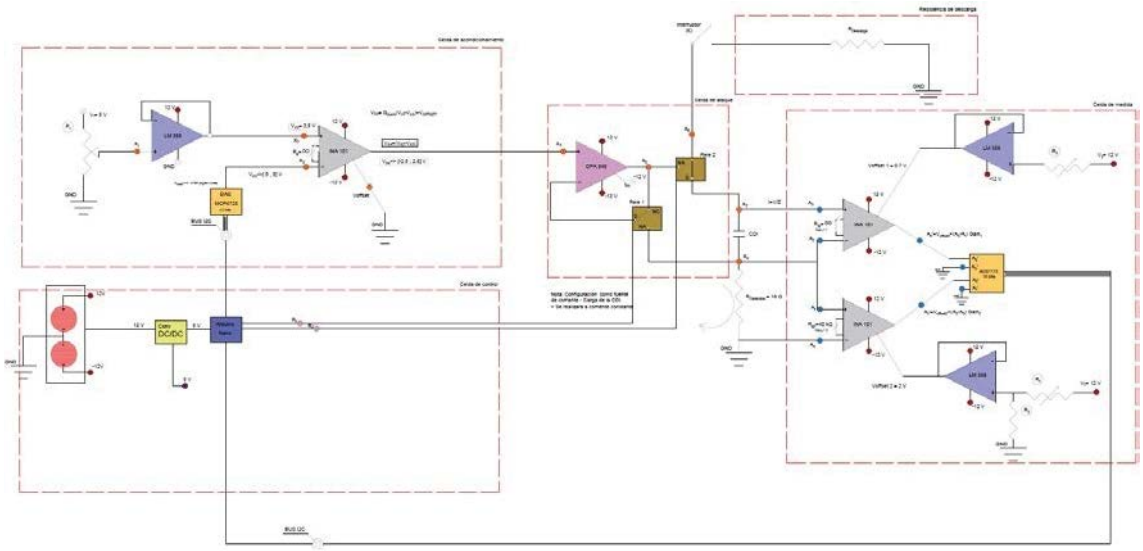

Fig. 2. Parts of the CCD prototype.

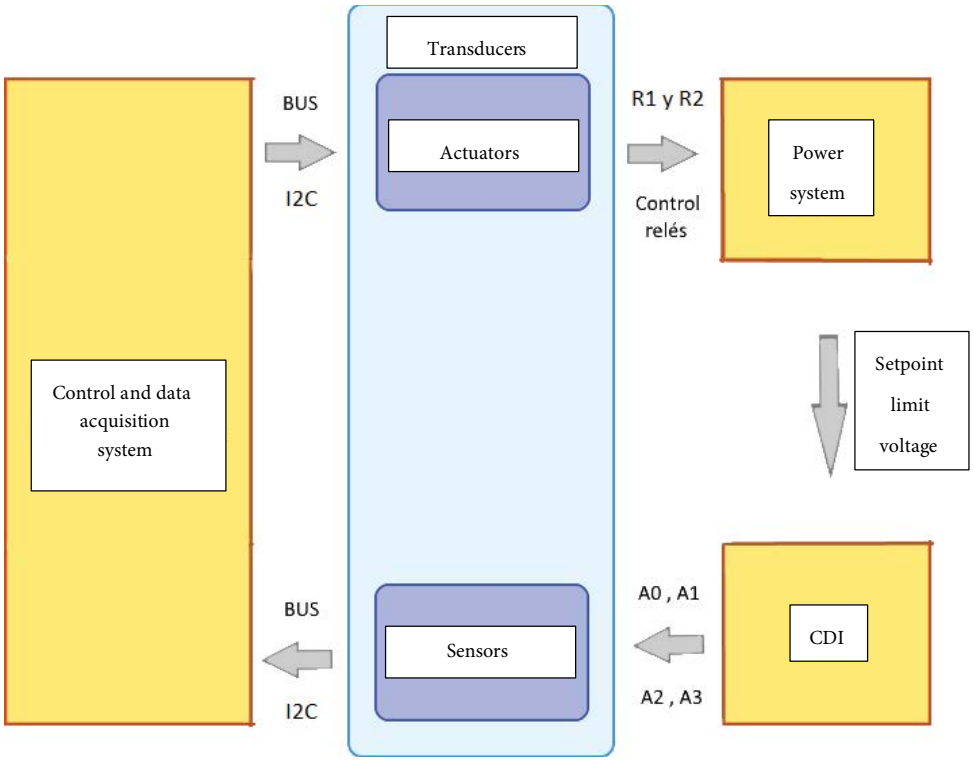

Fig. 3. Block diagram of the CCD system.

shall provide the load with a constant current at 95% efficiency and shall establish the duration for which the nominal voltage is maintained. The device shall be capable of measuring current and voltage with a maximum error tolerance of ±1%. Also, voltmeter measurements shall have a resolution of 0.125 mV for voltage measurement. The input impedance of these voltmeters must be sufficiently high for measurement errors to be negligible. To obtain the data, an analog-to-digital converter (ADC1115) has been used, which has a series of filters at the input and output of the converter, resulting in precise, noise-free data.

The designed device must be able to perform constant voltage and current charging and discharging, as well as simultaneous voltage and current measurements at the terminals of the CDI.

The power supply (through the OPA548T) must be able to provide the constant load current to the CDI with 95% efficiency and, in addition, set the duration of voltage maintenance.

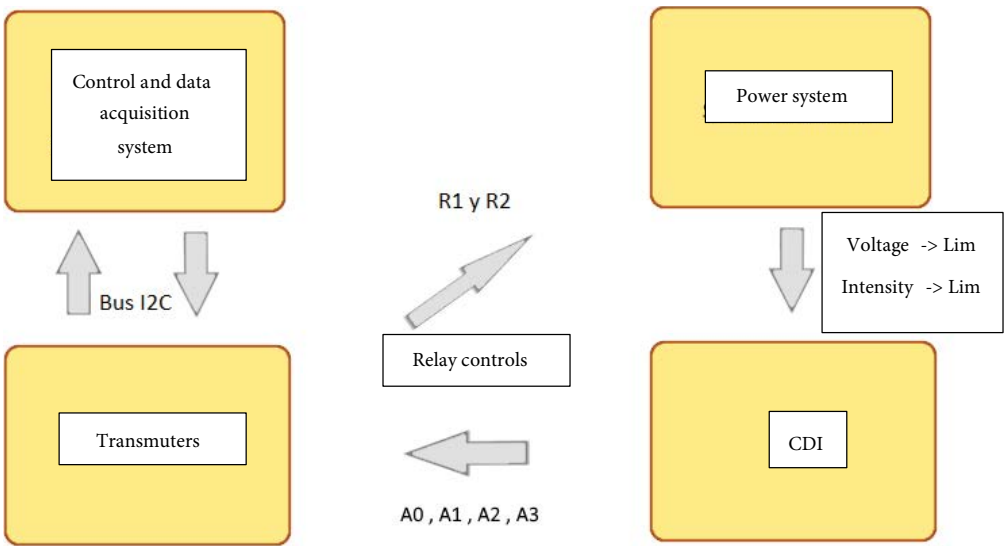

Fig. 4. Interrelation of blocks.

The developed device must satisfy the requirement of an error tolerance of ±0.01% for voltage measurement and an error tolerance of ±0.1% for current measurement.

3.1. Proposed test results

This section gives details of the tests carried out and the results obtained for the characterization of the CCD system.

3.1.1. Calibration of the equipment

To give veracity and reliability to the results obtained during the tests, the CCD prototype was first subjected to a series of calibration tests. The procedure followed consisted in the fact that, knowing an input setpoint, the system returned a series of expected results since the output data were known, since a 1 Ω resistor was used instead of a CCD cell.

3.1.1.1. Calibration of the digital-to-analog converter (MCP4725)

The first test of the CCD prototype was the calibration of the equipment by setting an input setpoint current to measure the voltage at the terminals of the 1 Ω resistor, see the results in Table 1. With this experience, the calibration line of the equipment is determined, obtaining the expression of the digital-to-analog converter's transformation of accounts.

As can be seen in Fig. 5, the slope of the straight line corresponds to the resistance of 1 Ω, and it can also be seen that the data dispersion is null, so the sample taken refers to the population and indicates that the CCD prototype is characterized with the Eq. (1):

$$y = 1.0588X + 3.9833 \quad (1)$$

where x is the rated set-point current in mA; y is the current at the load mA.

Table 1
Calibration of the system in the digital-to-analog converter (MCP4725)

I_c (mA)	Measures (mA)	
–138.890	–142.1	Test 1
–13.889	–10.6	
–1.3889	2.1	
0	3.9	
1.3889	5.6	
13.889	18.7	
138.890	151.5	
–138.890	–143.1	Test 2
–13.889	–10.5	
–1.3889	2.4	
0	3.6	
1.3889	5.3	
13.889	18.6	
138.890	151.4	
–138.890	–142.9	Test 3
–13.889	–10.5	
–1.3889	2.3	
0	3.7	
1.3889	5.4	
13.889	18.6	
138.890	151.4	

Finally, knowing the current, the voltage is trivial because the resistance is 1 Ω.

3.1.1.2. Calibration of the analog-to-digital converter (ADS1115)

This experiment is based on connecting a 1 Ω (Ohms) resistor to the load and establishing an input setpoint current

to measure the voltage in the measuring cell, with this we know the current and current of the CCD system, Fig. 6. With this experience, the calibration line of the equipment is determined, obtaining the expression of the transformation of accounts of the analog-to-digital converter.

As can be seen in Figs. 7–9, the data dispersion is null, so the sample taken refers to the population and indicates that the CCD prototype is characterized with the equations: (2) "I" of measured ADC counts, (3) is the sensor current, (4) "V" of measured ADC counts and (5) is the sensor voltage.

$$y = 141704X + 20340 \quad (2)$$

where x is the rated set point current in A; y is the counts corresponding to the current of the ADS1115.

$$y = 17.691X + 2.5387 \quad (3)$$

where x is the rated setpoint current in A; y is the measured current in V at the sensor;

$$y = -9466.1X + 5577.9 \quad (4)$$

where x is the rated setpoint current in A; y is the counts corresponding to the voltage of the ADS1115;

$$y = -1.1824X + 0.6963 \quad (5)$$

where x is the rated setpoint current in A; y is the measured voltage in V at the sensor.

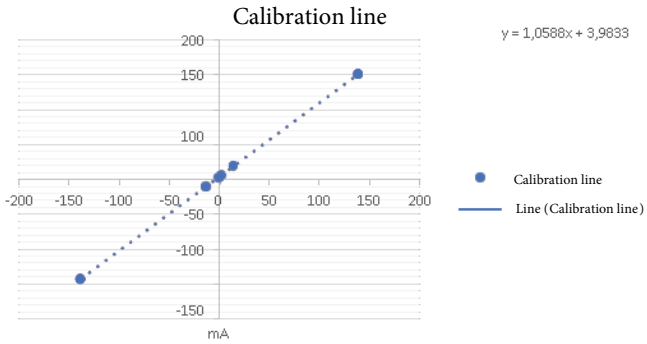

Fig. 5. Digital Analogical Converter calibration with the load resistance.

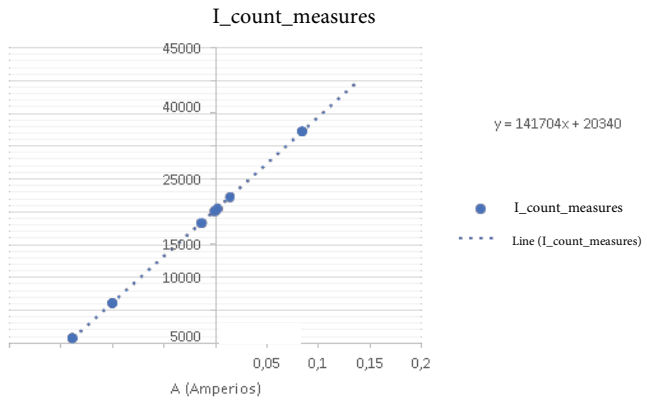

Fig. 6. "I" counts measured at the ADC.

3.1.2. Charging and self-discharge tests at an input set point

This section specifies the tests to which the equipment is subjected for its validation, where the degree of response of the equipment to an input setpoint will be determined, characterizing its behavior through the supercapacitors and the standardized tests.

Three samples were taken in each test to avoid uncertainty and mean error. Furthermore, the data obtained in the tests are representative of the CCD system.

The first characterization test performed was the charging and self-discharging of a 1 F capacity supercapacitor with a setpoint voltage of 2 V and a setpoint current of 0.1 A. The data generated were stored in a database. The data generated have been saved in a plain text file with ".txt" extension for further processing.

A script has been created with MATLAB software for data management on the screen. In this way, a detailed analysis of each test carried out is carried out. The result of this first test can be seen in Fig. 10.

Figs. 10 and 11 show that the test was carried out satisfactorily, although there is a small variation of 0.01 A in the current. This was due to an equipment calibration problem, hence the importance of having the CCD system properly calibrated.

The following tests were at the same maximum set point voltage, but at the set point current of 0.05 and 0.025 A, respectively. Figs. 12 and 13 show the results of the tests per screen.

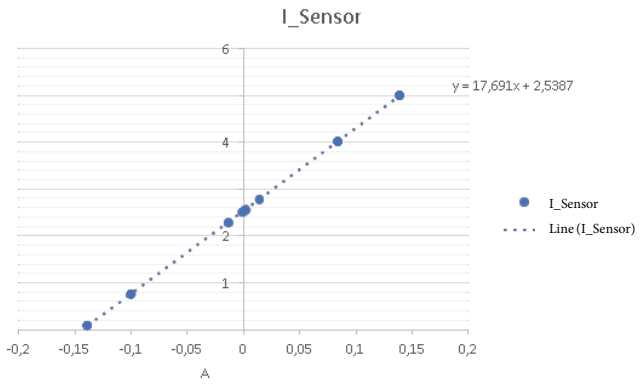

Fig. 7. Intensity at the sensor.

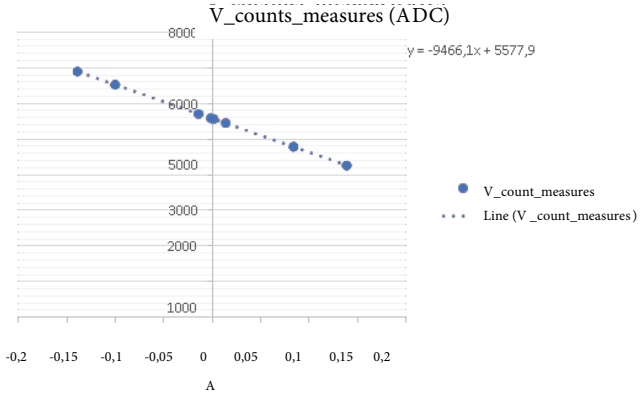

Fig. 8. "V" counts measured on the ADC.

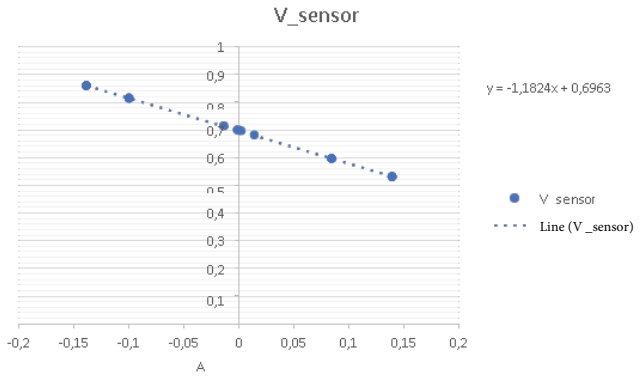

Fig. 9. Voltage at the sensor.

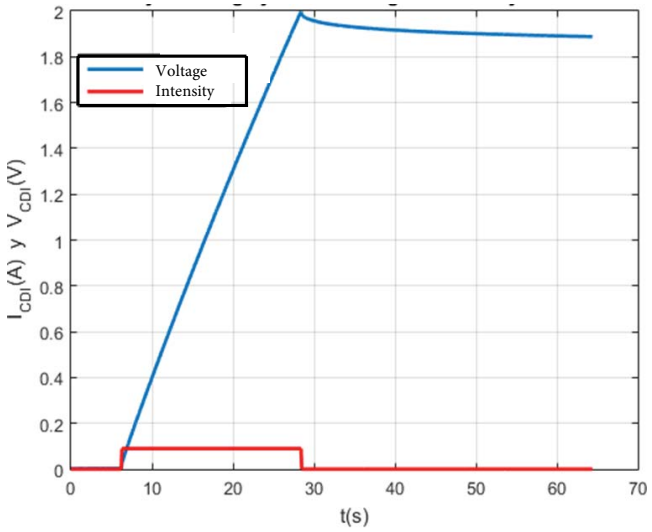

Fig. 10. Charging and self-discharge test at Vc_max = 2 V and I_c = 0.1 A.

On the other hand, the system was validated with another supercapacitor of capacity 650 F at another maximum voltage and setpoint current. The test results can be seen in Fig. 14.

Firstly, as can be seen in Fig. 14, the test was carried out at the set voltage of 0.4 V and set current of 0.1 A. This test lasted 1 h. It should be noted that the results are as expected for a supercapacitor with these characteristics, the reason being that the setpoint current is very small and the capacity of the supercapacitor is too large.

On the other hand, quality results have been obtained without the adverse effects of noise. This was possible because the design of the CCD system foresaw the need to have a noise-free reading of the data when characterizing. For this reason, the use of the analog-to-digital converter (ADS1115) is fundamental to the system. This converter has a series of input and output filters that result in accurate and noise-free data.

Finally, the self-discharge of the CCD for 1, 100 and 150 F supercapacitors has been analysed and characterized (Figs. 15–18). The results shown are satisfactory and, with this, the characterization system is again validated.

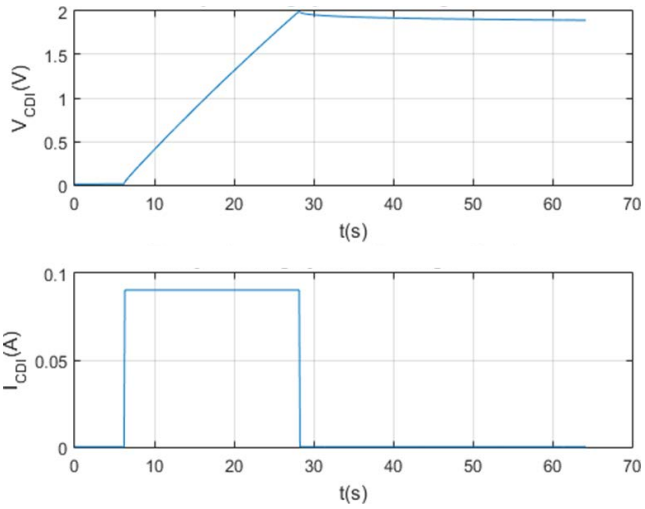

Fig. 11. Charge and self-discharge test (Voltage – Current) Vc_max = 2 V and I_c = 0.1 A.

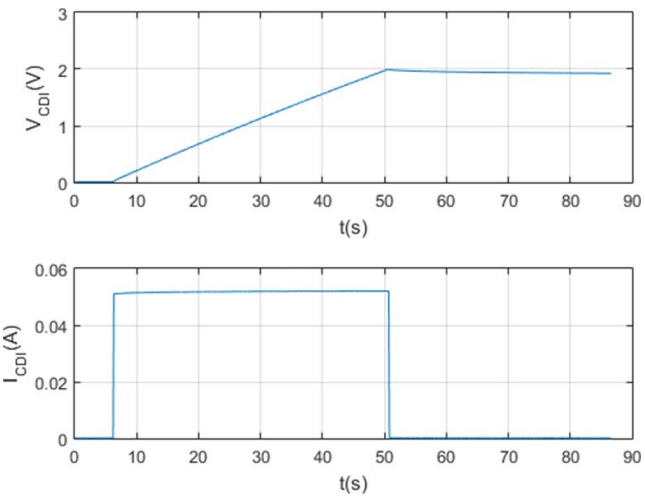

Fig. 12. Load and self-discharge test at Vc_max = 2 V and I_c = 0.05 A.

As can be seen in Fig. 19, there are anomalies at the beginning of the charge and self-discharge. It has been deduced from the results obtained that an equivalent series resistance coexists due to the poor connection of the supercapacitor with the system terminals, resulting in a series resistance of 56 Ω. This can be seen in more detail in Fig. 20.

3.1.3. CCD charging and discharging test

In this section, the system will be validated based on the standardized tests for supercapacitors. For the first charge and discharge characterization test of the CCD system, the initial data have been programmed via the interface created with processing. Table 3 shows the data given to the interface.

Once the data has been entered on the screen, the test is started. Once the test has been completed and the data

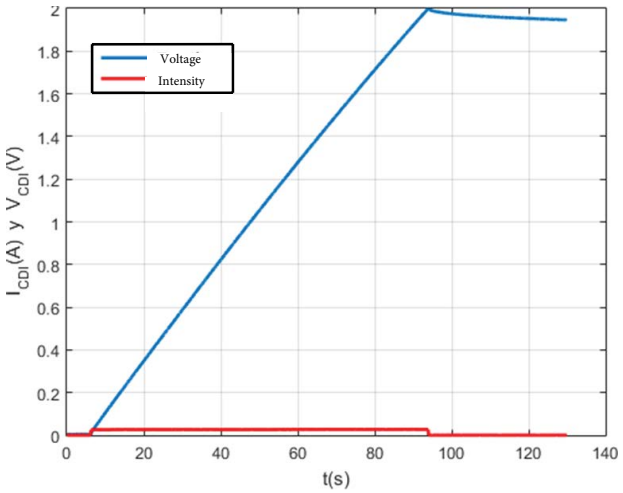

Fig. 13. Charge and self-discharge test at Vc_max = 2 V and I_c = 0.025 A.

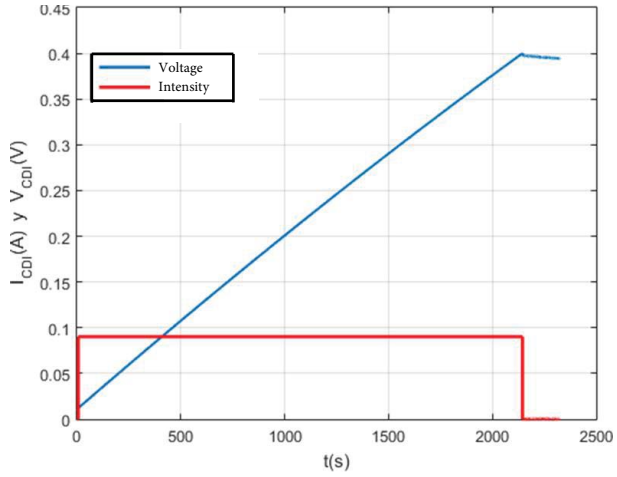

Fig. 14. Test with a 650 F supercapacitor.

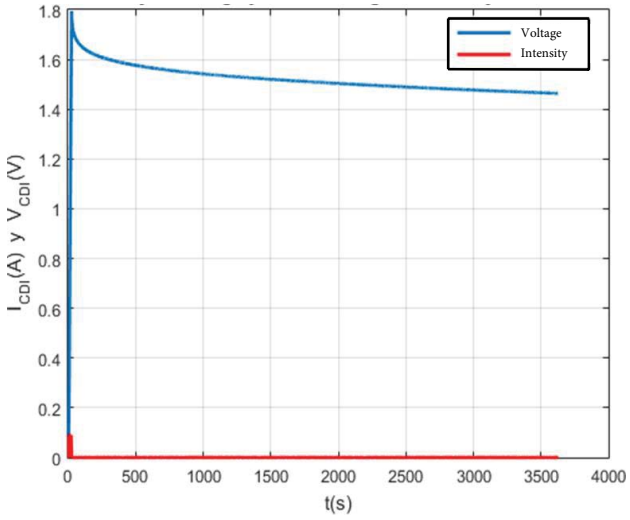

Fig. 15. Self-discharge test to characterize a 1 F capacitor.

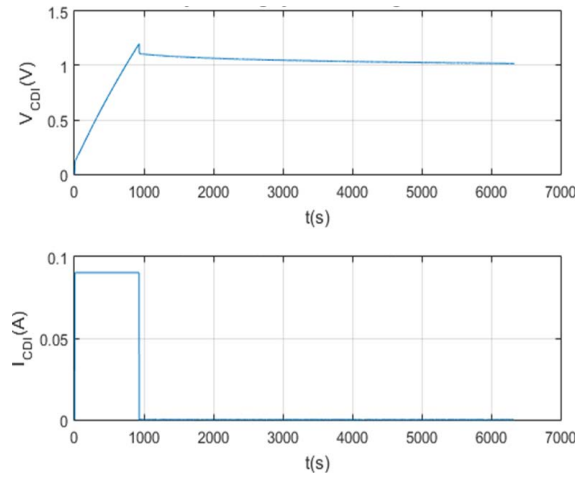

Fig. 16. Self-discharge analysis characterizing a 100 F capacitor.

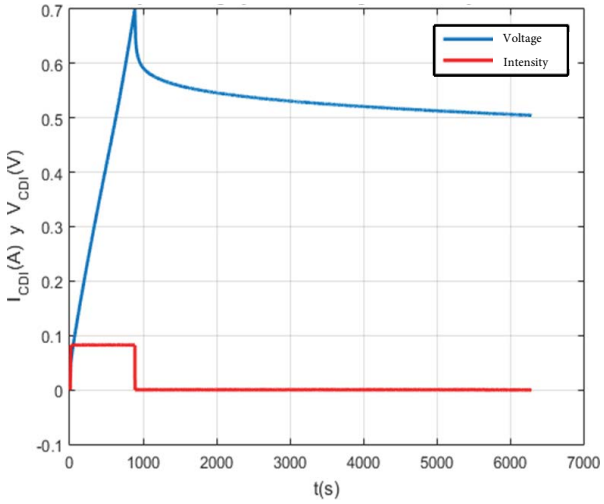

Fig. 17. Charge and self-discharge test to characterize a 150 F capacitor.

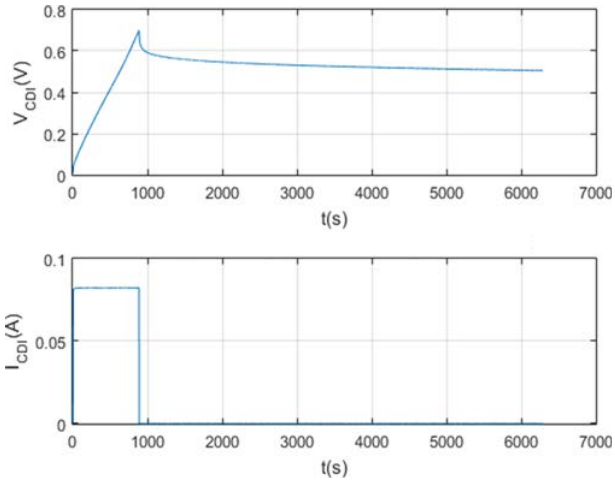

Fig. 18. Graph with details of the charge and self-discharge test characterizing it on a 150 F capacitor.

obtained has been managed, the result on the screen is shown in Fig. 19.

First, the test is satisfactory. Proof of this is the correlation with the behavior of the standardized tests, see chapter 3 of this study. Fig. 20 shows each of the times that make up the experiment, which are: time 1, time 2, time 3, time 4 and time 5.

Secondly, the test responds to the initially programmed times and the input setpoints (V_{cmax} and I_{con}).

Finally, the cleanliness of the data obtained should be highlighted, as the noise phenomenon in the result is negligible, Fig. 19. This has been possible with the analog-to-digital converter (ADS1115) which inhibits the noise generated by the instrumentation elements of the system.

Table 3
Data initially programmed in the processing interface

Time 1	0.3	Minutes
Time 2	45	Seconds
Time 3	0.025	Hours
Time 4	45	Seconds
Time 5	0.025	Hours
I_c	0.1	A (Amperes)
V_{cmax}	1.8	V (Volts)
Capacitor capacity	1	F (Farads)

On the other hand, another test has been carried out with different initial conditions to those described above to validate the CCD system. The data entered by the interface are shown in Table 4.

The results per screen can be seen in Fig. 21.

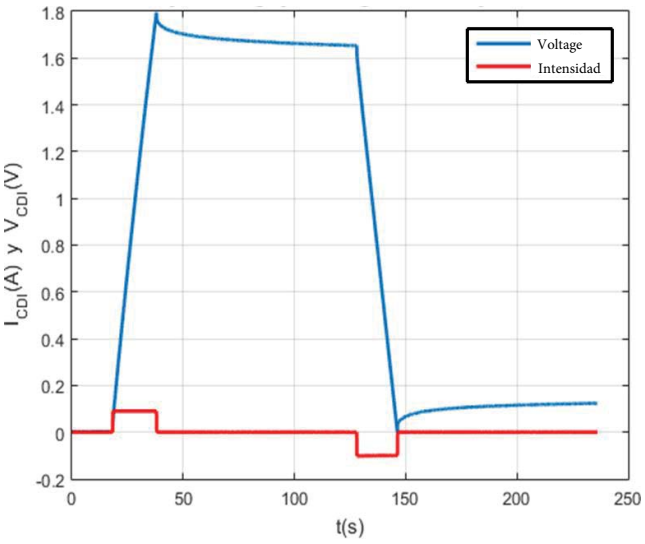

Fig. 19. Charge and discharge test at V_{cmax} = 1.8 V and I_{con} = 0.1 A.

Table 2
Calibration of the system in the analog-to-digital converter (ADS1115)

V_sensor	I_sensor	V_counts_measures	I_count_measures	Sample
0.860	0.091	6,892	735	Measure 1
0.816	0.757	6,527	6,060	
0.713	2.292	5,710	18,365	
0.698	2.515	5,591	20,152	
0.696	2.541	5,578	20,354	
0.695	2.563	5,565	20,535	
0.680	2.784	5,450	22,302	
0.597	4.020	4,785	32,260	
0.860	0.090	6,889	730	Measure 2
0.814	0.760	6,524	6,090	
0.713	2.290	5,710	18,346	
0.698	2.515	5,592	20,142	
0.696	2.542	5,578	20,358	
0.695	2.565	5,565	20,542	
0.680	2.783	5,450	22,290	
0.597	4.020	4,785	32,261	
0.860	0.090	6,887	730	Measure 3
0.814	0.761	6,524	6,100	
0.713	2.292	5,710	18,362	
0.698	2.515	5,592	20,145	
0.696	2.543	5,577	20,366	
0.695	2.565	5,567	20,546	
0.680	2.783	5,450	22,290	
0.597	4.020	4,786	32,260	

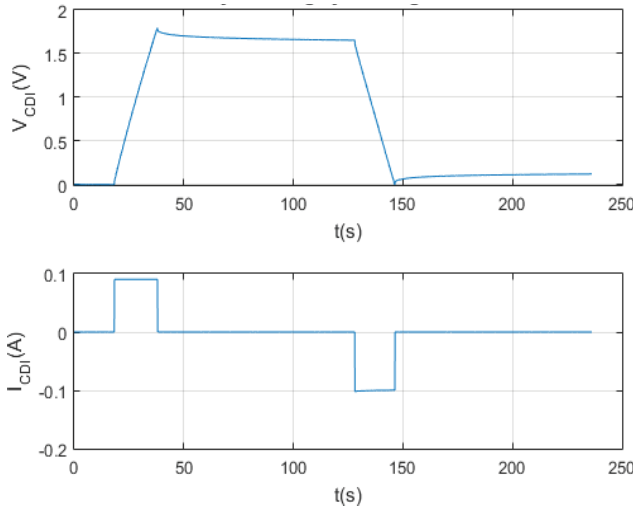

Fig. 20. Detailed graph for the loading and unloading test at V_{cmax} = 1.8 V and I_{con} = 0.1 A.

Table 4
Data programmed for the second loading and unloading test

Time 1	0.3	Minutes
Time 2	45	Seconds
Time 3	0.1	Hours
Time 4	45	Seconds
Time 5	0.1	Hours
I_c	0.1	A (Amperes)
V_{cmax}	2	V (Volts)
Capacitor capacity	1	F (Farads)

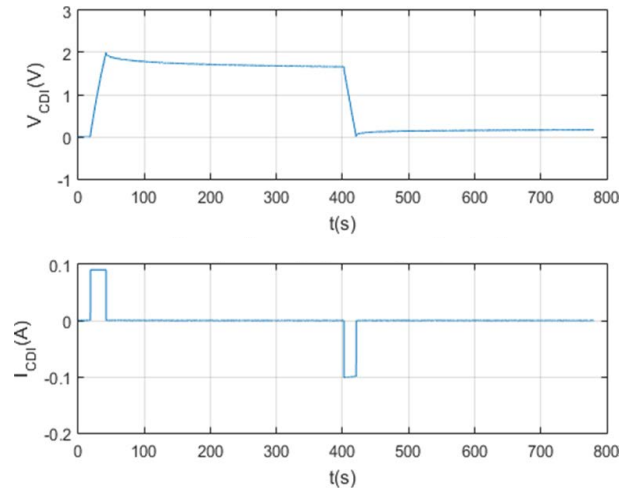

Fig. 21. Charge and discharge test for the 1 F supercapacitor with other input setpoints.

In Fig. 21, it can be seen in time interval 5 that the capacitor self-charges once this period starts. The cause is the inertia of the capacitor in maintaining an equilibrium state, even though the attack current in the CCD system is 0 A.

Table 5
Data programmed to characterize the CCD system

Time 1	1	Minutes
Time 2	45	Seconds
Time 3	0.025	Hours
Time 4	45	Seconds
Time 5	0.025	Hours
I_c	0.1	A (Amperes)
V_{cmax}	1	V (Volts)
Capacitor capacity	1	F (Farads)

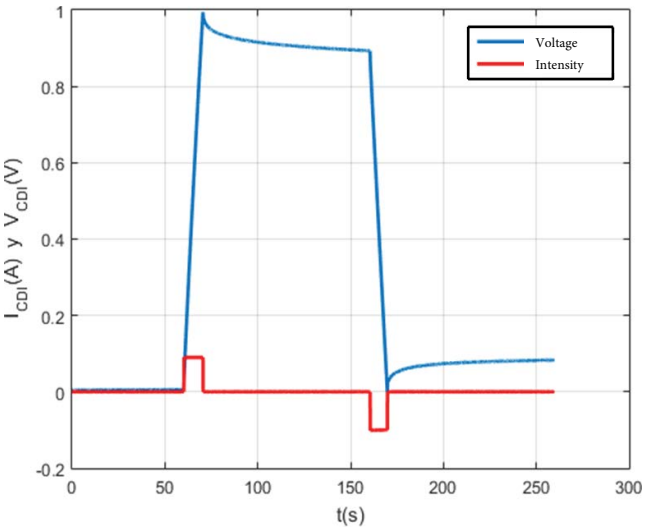

Fig. 22. Charging and discharging test characterizing a 1 F supercapacitor.

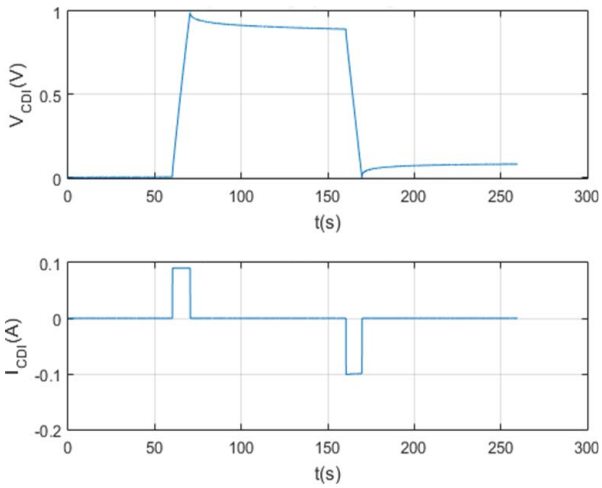

Fig. 23. Charge and discharge test at V_{cmax} = 1 V and I_{con} = 0.1 A.

Finally, a new charge-discharge test is carried out with a supercapacitor of capacity 1 F (Farad), with different initial conditions to those previously described. The data initially programmed by the interface are shown in the following Table 5.

Figs. 22 and 23 show the results of the test per screen.

4. Conclusions

The conclusions obtained in the development of this study are as follows:

(1) A prototype has been designed that can operate with constant current charging and discharging.
(2) Adequate precision has been achieved, as can be seen in the results obtained.
(3) A philosophy of using free software with open-source code has been followed, such as: the Arduino and Processing Programming Editors; as well as the Arduino Nano Board, the analog-to-digital converter and the Adafruit digital-to-analog converter.
(4) A low-cost system has been developed.
(5) A robust and versatile system has been designed for water treatment.
(6) A flexible system has been obtained for the specifications established.

Acknowledgments

This research was co-funded by the UNIDIGITAL - PIEFI - Línea 3. Contenidos y programas de formación. Código del proyecto PIE 2022-60 "Laboratorios como entornos de trabajo para el aprendizaje activo y colaborativo mediante el diseño, desarrollo, construcción, utilización y el rediseño de equipos y dispositivos para su aplicación en las prácticas".

References

[1] M. Kurihara, Seawater reverse osmosis desalination, Membranes, 11 (2021) 243, doi: 10.3390/membranes11040243.
[2] A. Ruiz-García, N. Melián-Martel, I. Nuez, Short review on predicting fouling in RO desalination, Membranes, 7 (2017) 62, doi: 10.3390/membranes7040062.
[3] F. Leon, A. Ramos, J. Vaswani, C. Mendieta, S. Brito, Climate change mitigation strategy through membranes replacement and determination methodology of carbon footprint in reverse osmosis RO desalination plants for islands and isolated territories, Water, 13 (2021) 293, doi: 10.3390/w13030293.
[4] P. Simon, Ed., Tapped Out: The Coming World Crisis in Water and What We Can Do About It, Rain Publishers, New York, 1988.
[5] M.A. Anderson, A.L. Cudero, J. Palma, Capacitive deionization as an electrochemical means of saving energy and delivering clean water. Comparison to present desalination practices: will it compete?, Electrochim. Acta, 55 (2010) 3845–3856.
[6] J.W. Blair, G.W. Murphy, Saline water conversion, 27 (1960) 206–223.
[7] A.M. Johnson, A.W. Venolia, R.G. Wilbourne, J. Newman, C.M. Wong, W. Sherman Gillam, S. Johnson, R.H. Horowitz, The Electrosorb Process for Desalting Water, Research and Development Progress Report No. 516, United States Department of the Interior, Washington, 1970.
[8] A.M. Johnson, J. Newman, Desalting by means of porous carbon electrodes, J. Electrochem. Soc., 118 (1971) 510, doi: 10.1149/1.2408094.
[9] Y. Oren, A. Soffer, Electrochemical parametric pumping, J. Electrochem. Soc., 125 (1978) 869, doi: 10.1149/1.2131570.
[10] D.D. Caudle, J.H. Tucker, J.L. Cooper, B.B. Arnold, A. Papastamataki, Electrochemical Demineralization of Water with Carbon Electrodes, United States Department of the Interior, Washington, 1966.
[11] H.M.N. AlMadani, Water desalination by solar powered electrodialysis process, Renewable Energy, 28 (2003) 1915–1924.
[12] M. del Pilar Mier López, R.I. Mendizábal, I.O. Uribe, M.J.R. Martínez, Electrodiálisis con membranas bipolares: fundamentos y aplicaciones, Ing. Chim., 418 (2004) 166–182.
[13] S. Porada, R. Zhao, A. van der Wal, V. Presser, P.M. Biesheuvel, Review on the science and technology of water desalination by capacitive deionization, Prog. Mater Sci., 58 (2013) 1388–1442.
[14] J.-B. Lee, K.-K. Park, H.-M. Eum, C.-W. Lee, Desalination of a thermal power plant wastewater by membrane capacitive deionization, Desalination, 196 (2006) 125–134.
[15] H. Li, Y. Gao, L. Pan, Y. Zhang, Y. Chen, Z. Sun, Electrosorptive desalination by carbon nanotubes and nanofibres electrodes and ion-exchange membranes, Water Res., 42 (2008) 4923–4928.
[16] P.M. Biesheuvel, A. van der Wal, Membrane capacitive deionization, J. Membr. Sci., 346 (2010) 256–262.
[17] Y.-J. Kim, J.-H. Choi, Improvement of desalination efficiency in capacitive deionization using a carbon electrode coated with an ion-exchange polymer, Water Res., 44 (2010) 990–996.
[18] P.M. Biesheuvel, R. Zhao, S. Porada, A. van der Wal, Theory of membrane capacitive deionization including the effect of the electrode pore space, J. Colloid Interface Sci., 360 (2011) 239–248.
[19] Y. Bouhadana, M. Ben-Tzion, A. Soffer, D. Aurbach, A control system for operating and investigating reactors: the demonstration of parasitic reactions in the water desalination by capacitive de-ionization, Desalination, 268 (2011) 253–261.
[20] O.N. Demirer, R.M. Naylor, C.A. Rios Perez, E. Wilkes, C. Hidrovo, Energetic performance optimization of a capacitive deionization system operating with transient cycles and brackish water, Desalination, 314 (2013) 130–138.
[21] P. Długołęcki, A. van der Wal, Energy recovery in membrane capacitive deionization, Environ. Sci. Technol., 47 (2013) 4904–4910.
[22] M.E. Suss, T.F. Baumann, W.L. Bourcier, C.M. Spadaccini, K.A. Rose, J.G. Santiago, M. Stadermann, Capacitive desalination with flow-through electrodes, Energy Environ. Sci., 5 (2012) 9511–9519.
[23] Y. Bouhadana, E. Avraham, M. Noked, M. Ben-Tzion, A. Soffer, D. Aurbach, Capacitive deionization of NaCl solutions at non-steady-state conditions: inversion functionality of the carbon electrodes, J. Phys. Chem. C, 115 (2011) 16567–16573.
[24] S.-i. Jeon, H.-r. Park, J.-g. Yeo, S.C. Yang, C.H. Cho, M.H. Han, D.K. Kim, Desalination *via* a new membrane capacitive deionization process utilizing flow-electrodes, Energy Environ. Sci., 6 (2013) 1471–1475.
[25] J.W. Blair, G.W. Murphy, Electrochemical Demineralization of Water with Porous Electrodes of Large Surface Area, In: Saline Water Conversion, American Chemical Society, New York, 1960, pp. 206–223.
[26] B.B. Arnold, G.W. Murphy, Studies on the electrochemistry of carbon and chemically-modified carbon surfaces, J. Phys. Chem., 65 (1961) 135–138.
[27] G.W. Murphy, J.L. Cooper, J.A. Hunter, Activated Carbon Used as Electrodes in Electrochemical Demineralization of Saline Water, United States Department of the Interior, Washington, 1969.
[28] G.W. Murphy, D.D. Caudle, Mathematical theory of electrochemical demineralization in flowing systems, Electrochim. Acta, 12 (1967) 1655–1664.
[29] S. Evans, W.S. Hamilton, The mechanism of demineralization at carbon electrodes, J. Electrochem. Soc., 113 (1966) 1314, doi: 10.1149/1.2423813.
[30] S. Evans, M.A. Accomazzo, J.E. Accomazzo, Electrochemically controlled ion exchange, J. Electrochem. Soc., 116 (1969) 307–309.
[31] G.W. Reid, F.M. Townsend, A.M. Stevens, Field Operation of a 20 Gallons Per Day Pilot Plant Unit for Electrochemical Desalination of Brackish Water, University of Michigan Library, 1968
[32] A.I. Beliakov, A.M. Brintsev, 7th International Seminar on Double Layer Capacitors and Similar Energy Storage Devices,

Florida Educational Seminars, Inc., Deerfield Beach (FL), December 1997.
[33] L. Zubieta, R. Bonert, Characterization of Double-Layer Capacitors for Power Electronics Applications, IEEE Transactions on Industry Applications, IEEE, 2000, pp. 199–205.
[34] A. Lasia, Electrochemical Impedance Spectroscopy and Its Applications, Modern Aspects of Electrochemistry, Kluwer Academic/Plenum Publishers, New York, 1999.
[35] S. Buller, E. Karden, D. Kok, R.W. De Doncker, Modeling the dynamic behavior of supercapacitors using impedance spectroscopy, IEEE Trans. Ind. Appl., 38 (2002) 1622–1626.
[36] C. Schiller, Main error sources at AC measurements, Electrochem. Appl., 1 (1997) 10–11.
[37] EN 62391-1:2006, Condensadores eléctricos fijos de doble capa para su uso en equipos electrónicos. Parte 1: Especificación genérica (IEC 62391-1:2006) (Ratificada por AENOR en septiembre de 2006), 2006.
[38] EN 62391-2-1:2006, Condensadores eléctricos fijos de doble capa para su uso en equipos electrónicos. Parte 2-1: Especificación marco particular: Condensadores eléctricos de doble capa para aplicación de potencia. Nivel de evaluación EZ (IEC 62391-2-1:2006), 2006.
[39] EN 62391-2:2006, Condensadores eléctricos fijos de doble capa para su uso en equipos electrónicos. Parte 2: Especificación intermedia: Condensadores eléctricos de doble capa para aplicación de potencia (IEC 62391-2:2006) (Ratificada por AENOR en septiembre de 2006), 2006.
[40] EN 62576:2010, Condensadores eléctricos fijos de doble capa para vehículos eléctricos híbridos. Métodos de ensayo de las características eléctricas. (Ratificada por AENOR en febrero de 2011), 2010.
[41] H. Gualous, D. Bouquain, A. Berthon, J.M. Kauffmann, Experimental study of supercapacitor serial resistance and capacitance variations with temperature, J. Power Sources, 123 (2003) 86–93.
[42] H. El Brouji, J.-M. Vinassa, O. Briat, N. Bertrand, E. Woirgard, Ultracapacitors Self-Discharge Modelling Using a Physical Description of Porous Electrode Impedance, 2008 IEEE Vehicle Power and Propulsion Conference, IEEE, Harbin, China, 2008.
[43] W.G. Pell, B.E. Conway, Analysis of power limitations at porous supercapacitor electrodes under cyclic voltammetry modulation and DC charge, J. Power Sources, 96 (2001) 57–67.
[44] F. Fabregat-Santiago, I. Mora-Seró, G. Garcia-Belmonte, J. Bisquert, Cyclic voltammetry studies of nanoporous semiconductors. capacitive and reactive properties of nano-crystalline TiO_2 electrodes in aqueous electrolyte, J. Phys. Chem. B, 107 (2003) 758–768.
[45] A. Burke, J. Miller, Testing of electrochemical capacitors: capacitance, resistance, energy density and power capability, Electrochim. Acta, 55 (2010) 7538–7548.
[46] R.R. Martín Hernández, Análisis, Modelado e Identificación de los Condensadores Electroquímicos de Doble Capa, Tesis Doctoral, 2014.
[47] Texas Instruments, OPA548 High-Voltage, High-Current Operational Amplifier. Available at: http://www.ti.com/lit/ds/symlink/opa548.pdf (May 2018).
[48] Arduino, Arduino Nano. Available at: https://store.arduino.cc/usa/arduino-nano (March 2018).
[49] BQ, Arduino Nano Pinout. Available at: https://www.bq.com/es/ (April 2018).
[50] Spark Fun Electronics, MCP4725. Available at: https://www.sparkfun.com/datasheets/BreakoutBoards/MCP4725.pdf (April 2018).
[51] Adafruit, MCP4725 Breakout Board – 12-Bit DAC w/I2C Interface. Available at: https://www.adafruit.com/product/935 (June 2018).
[52] Texas Instruments, ADS111x Ultra-Small, Low-Power, I2C-Compatible, 860-SPS, 16-Bit ADCs With Internal Reference, Oscillator, and Programmable Comparator, Available at: http://www.ti.com/lit/ds/symlink/ads1115.pdf (May 2018).
[53] Adafruit, ADS1115 16-Bit ADC - 4 Channel with Programmable Gain Amplifier. Available at: https://www.adafruit.com/product/1085 (June 2018).
[54] Texas Instruments, High Accuracy Instrumentation Amplifier. Available at: http://www.ti.com/lit/ds/sbos133/sbos133.pdf (March 2018).
[55] Analog Devices, ADM3260. Available at: http://www.analog.com/en/products/interface-isolation/isolation/isopower/adm3260.html#product-overview (June 2018).
[56] Texas Instruments, OPA549 High-Voltage, High-Current Operational Amplifier. Available at: http://www.ti.com/lit/ds/symlink/opa548.pdf (June 2018).
[57] R. Zhao, P.M. Biesheuvel, A. van der Wal, Energy consumption and constant current operation in membrane capacitive deionization, Energy Environ. Sci., 5 (2012) 9520–9527.